*Snežana Marković[1], Bojana Radojković[2], Bore Jegdić[2], Aleksandar Jovanović[3], Jovica Stojanović[3], Milan Trumić[1], Vaso Manojlović[4]**

[1]University of Belgrade, Technical Faculty in Bor, Bor, Serbia, [2]University of Belgrade, Institute for Chemistry, Technology and Metallurgy, Belgrade, Serbia, [3]Institute for Technology of Nuclear and Other Mineral Raw Materials, Belgrade, Serbia, [4]University of Belgrade, Faculty of Technology and Metallurgy, Belgrade, Serbia

Scientific paper
ISSN 0351-9465, E-ISSN 2466-2585
https://doi.org/10.62638/ZasMat998

Zastita Materijala 65 (1)
45 - 53 (2024)

Corrosion behavior of high- and low-chromium steel grinding balls in chloride solution

ABSTRACT

The corrosion behaviour of three types of alloys (two low-alloy carbon steel and one stainless iron with ~15 wt.% Cr), in a solution which simulates seawater (3% NaCl solution, pH 8.1) was tested. Tested samples are used to make steel (iron) balls applied in mils for grinding copper and other ore. The corrosion tests were performed using three electrochemical methods, at room temperature in the presence of atmospheric oxygen. The linear polarization resistance (LPR) method, electrochemical impedance spectroscopy (EIS) method, and linear sweep voltammetry (LSV) method were applied. Based on measurements by LPR and EIS methods (as non-destructive methods), the value of polarization resistance (R_p) was determined and the general corrosion rate (v_{corr}) of the examined samples was calculated. The obtained values of the general corrosion rate can be used to calculate the service life of steel (iron) balls under exploitation conditions (seawater). The appearance of the surface after linear sweep voltammetry (LSV) measurement showed the presence of localized corrosion (pits were formed) of the tested samples, especially stainless iron, and the LSV method is not suitable for the determination of the general corrosion rate of tested samples in seawater. This form of corrosion occurs at high anodic polarizations, during performing LSV measurements.

Keywords: *Low-alloy Steel, Stainless Iron, Electrochemical Corrosion, LPR, EIS, LSV, Seawater*

1. INTRODUCTION

Steel balls used for grinding copper and other ores during exploitation are exposed to intense wear and corrosion. Corrosion processes are very important considering that steel balls and ore are in contact with seawater. The procedure for determination of the level of synergetic action wear and corrosion is analysed in the ASTM G119 standard [1].

In seawater, during electrochemical corrosion, on the steel surface, two electrochemical reactions (anodic and cathodic) occur simultaneously. The anodic reaction is the dissolution of the metal (steel), i.e. the transition of metal ions into the solution. The cathodic reaction is the reduction of oxygen dissolved in seawater. The oxygen present in the seawater removes electrons from the metal surface, ensuring the transition of the metal atom to the ionic state.

*Corresponding author: Vaso Manojlović
E-mail: v.manojlovic@tmf.bg.ac.rs
Paper received: 14. 09. 2023.
Paper accepted: 12. 10. 2023.
Paper is available on the website: www.idk.org.rs/journal

In accordance with the heterogeneous theory of electrochemical corrosion, the places where the anodic and cathodic reactions take place on the metal surface are separated and the flow of electrons in the metal is necessary for the occurrence of the corrosion processes. Such a separation of anodic and cathodic reactions is energetically favourable. General corrosion is characterized by a uniform reduction in metal thickness, without significant localized attack. During the occurrence of general corrosion, the anodic and cathodic sites are replaced, as a result of which the dissolution of the steel is approximately the same over the entire surface of the metal [2].

A quantitative indicator of general corrosion is its corrosion rate. The rate of corrosion can be determined in the exploitation conditions [3, 4], at corrosion stations [4-6], based on mass loss of the specimens before and after corrosion tests [7-9], in the different chambers such as a chamber with neutral salt spray, a chamber with acid-salt spray [10], etc. The mentioned methods require a long time to obtain appropriate results. The rate of general corrosion is presented by the depth of the

corrosion into metal for a certain period and is most often expressed in mm year^{-1}.

In the last decades, electrochemical methods have been increasingly used to determine the corrosion rate of metals. As a result of electrochemical measurements, the polarization resistance and corrosion current density are obtained, on which value of the corrosion rate can be calculated.

In this work, the rate of general corrosion of three types of alloys (two low-alloyed carbon steels and one stainless iron with ~ 15 wt.% Cr) was determined. The tests were performed in a slightly alkaline 3% NaCl solution (pH 8.1), which simulates seawater, using several electrochemical methods. The electrochemical polarization resistance (LPR) method [11-14], the electrochemical impedance spectroscopy (EIS) method [15-18], and the linear sweep voltammetry (LSV) method [19-22], were applied.

With increasing the concentration of NaCl in the solution up to 3%, the solution conductivity increases. At the same time, the rate of steel corrosion also increases. On the other hand, at higher concentrations of NaCl, the solubility of the atmospheric oxygen decreases and the corrosion rate decreases [23]. Accordingly, the highest corrosion rate of the steel is in a 3% NaCl solution. This is the reason for the application of a 3% NaCl solution for performing experiments in this study.

Before the electrochemical corrosion measurements, the specimens (steel) were kept in the tested solution (3% NaCl solution, pH 8.1) for a certain time, at an open circuit potential, until a stable value of that potential was established. The open circuit potential is known as the mixed potential or corrosion potential for a given metal/electrolyte system. Corrosion potential is a basic indicator of the state of the corrosion system and it is a basis for subsequent electrochemical corrosion tests using the aforementioned methods.

The corrosion potential value can be used independently of other electrochemical measurements, as in the case of determining the condition of steel reinforcement in concrete. Steel reinforcement in concrete that is in a passive state has a corrosion potential value that is several hundred millivolts more positive than reinforcement that is in an active state, i.e., corroding reinforcement [24]. Also, the value of the corrosion potential of metals and alloys in a corrosive environment is used to predict the occurrence of galvanic corrosion [25-27]. A large number of different applications of corrosion potential measurement are summarized in the ASTM G215 standard [28] and literature [29, 30].

This paper aims to consider the possibility of determining the general corrosion rate of steel in a 3 % NaCl solution using different electrochemical methods. Also, based on the obtained values for the corrosion rate, the goal is to predict the reduction of the wall thickness of the steel balls (which are used for grinding copper or other ore), as well as the determination of the service life of the steel (iron) balls under the specified exploitation conditions.

2. MATERIALS AND METHODS

2.1. Materials

The chemical composition of the tested samples was determined by the optical emission spectrometer for metal analysis, Belec lab 3000s (Belec Spectrometric Opto-Elektronik GmbH, Germany) and is given in Table 1. S1 is casted steel, and contains < 0.1% chromium, S2 is steel in a wrought state and contains ~ 0.5% chromium, while S3 is casted iron and contains ~ 15 wt.% chromium. For the steels (iron) to be stainless, the chromium content must be greater than ~ 12 wt. %. Accordingly, S3 is stainless cast iron, because the carbon content in this sample is 2.56 wt. %.

Table 1. Chemical composition of the tested samples (wt.%)

Tabela 1. Hemijski sastav ispitanih uzoraka (mas. %)

	C	Si	Mn	P	S	Cu	Cr	Ni	Mo	Fe
S1	0.445	0.355	0.765	0.013	0.035	0.17	0.08	0.048	0.08	Rest
S2	0.74	0.42	0.667	0.008	0.005	0.049	0.51	0.033	0.013	Rest
S3	2.56	0.61	0.483	0.03	0.024	0.055	15.14	0.11	0.03	Rest

Table 2 lists the hardness values (HB), measured on a Brinell hardness testing machine. The Brinell hardness test was measured by pressing a hard steel ball (5 mm) into tested specimens with a 750 kg force for 20 seconds (AMSLER, Switzerland) and then measuring the size of the indentation by optical microscopy. The hardness value is the highest for S3 (iron with the highest concentration of carbon and chromium), and the lowest for the steel with the lowest concentration of carbon and chromium (steel S1). The hardness of steel S2 is higher than for S1, due

to its hardening structure formed during steel ball rolling.

Table 2. The hardness of the tested samples (HB)

Tabela 2. Tvrdoća ispitivanih uzoraka (HB)

	HB
S1	285
S2	547
S3	555

Before the electrochemical corrosion measurements, test specimens were cut from steel (iron) balls (the diameter of the balls was ~70 mm), and then successively grinded with grind paper with a fineness of 400 grit to 1000 grit. The specimens were washed with distilled water and dried. Until the beginning of the corrosion measurements, the specimens were kept in a desiccator.

A test solution (3% NaCl solution, pH 8.1) which simulates seawater was made using bi-distilled water and analytical grade NaCl. Natural seawater has a pH of 8.1 due to the presence of dissolved basic minerals, such as various carbonates. During the Industrial Revolution, due to the presence of acid rain, the pH value of seawater decreased from 8.2 to 8.1.

2.2. Linear polarization resistance (LPR)

The LPR method was used to determine the value of polarization resistance (R_p) of the tested samples in a corrosive environment (3% NaCl solution, pH 8.1). The R_p value is inversely proportional to the corrosion current density (j_{corr}), and the corrosion rate (v_{corr}). The steel in the solution was polarized in a narrow potential range (E = ± 10 mV) concerning the corrosion potential (E_{corr}), starting from the cathodic to the anodic potential values, and the corresponding current (j) was registered. The applied potential sweep rate was 0.5 mV s^{-1}. The polarization resistance was determined as the slope of the experimental curve E–j, at the corrosion potential. Based on the experimentally determined R_p value, the corrosion current density, and general corrosion rate of the samples were calculated.

2.3. Electrochemical impedance spectroscopy (EIS)

The EIS method also allows the determination of the value of the polarization resistance (R_p). A small amplitude alternating potential (± 10 mV vs. E_{corr}) was applied to the tested steel in the test solution. The range of applied frequencies (f) was from 100 000 Hz to 0.01 Hz. Based on the value of electrochemical impedance at very high and very low frequencies, the value of polarization resistance (R_p) was determined. The corrosion current density and the corrosion rate were calculated on the base measured R_p values.

The corrosion current density (j_{corr}) was calculated based on the value of the polarization resistance (R_p), using the Stern–Geary equation [31, 32]:

$$j_{corr} = B/R_p \quad (1)$$

Where

B is a constant that depends on the value of the anodic (b_a) and cathodic (b_c) Tafel slopes:

$$B = b_a \cdot b_c/(2.3 \cdot (b_a + b_c)) \quad (2)$$

Tafel slopes can be determined experimentally, by forming polarization Tafel diagrams, or their values can be taken from the literature [11]. For carbon steel in seawater, the value of the constant B is ~ 25 mV. Therefore, the corrosion current density (j_{corr}) is:

$$j_{corr} = 25\ mV/R_p \quad (3)$$

The corrosion rate of the tested samples (v_{corr} in mm yr^{-1}) was calculated using Faraday law, based on the obtained value of the corrosion current density (j_{corr} in µA cm^{-2}), in accordance with the ASTM G102 standard [32]:

$$v_{corr} = 0.01166 \cdot j_{corr} \quad (4)$$

2.4. Linear sweep voltammetry (LSV)

Tafel diagrams are obtained by this method. The steel in the 3% NaCl solution was polarized in the potential range E = ± 0.250 V in relation to the corrosion potential (E_{corr}) and the corresponding value of the current density (j) was registered. The applied potential sweep rate was 0.5 mV s^{-1}. From the obtained polarisation diagrams (E–log j), the corrosion current density (j_{corr}) was determined by extrapolation of the Tafel region of the anodic polarization curve to the corrosion potential (E_{corr}).

All electrochemical tests were performed using a potentiostat/galvanostat BioLogic SP-200, in a 3% NaCl solution (pH 8.1). Tests were performed at room temperature, in the presence of atmospheric oxygen.

The tests were carried out in a classical three-electrode electrochemical cell with a saturated calomel electrode (SCE) as a reference electrode and a Pt grid as an auxiliary electrode. The working electrode was the tested specimens, with a working surface of 1 cm^2. Before starting the electrochemical measurements, each specimen was held in the test solution for a certain time at the open circuit potential (up to 1 h), until a relatively stable corrosion potential (E_{corr}) was established.

2.5. Optical microscopy

The morphology of the surface of tested samples after polarization measurements (linear sweep voltammetry (LSV) method) was analysed by applying optical microscopy Carl Zeiss-Jena, JENAPOL-U polarizing microscope for reflected and transmitted light. The microscope was outfitted with a "Carl Zeiss AxioVision SE64 Rel. 4.9.1." software package, a "Multiphase" module, and an "Axiocam 105 color" camera.

3. RESULTS AND DISCUSSION

3.1. Corrosion potential (E_{corr})

The tested specimens were kept in a 3% NaCl solution at an open circuit potential until a relatively stable corrosion potential was established. In the initial period of exposure, there was a relatively rapid decrease in the value of the corrosion potential (Figure 1).

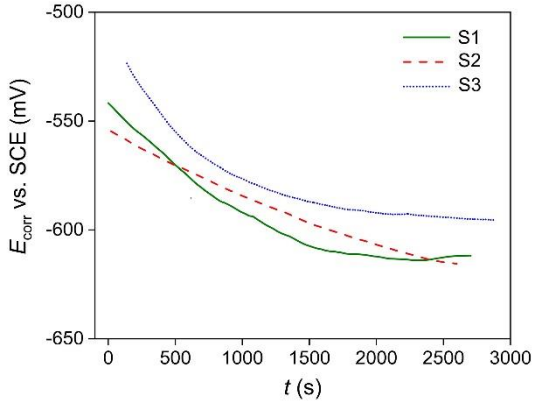

Figure 1. Time dependence of the corrosion potential for samples S1, S2, and S3

Slika 1. Zavisnost korozionog potencijala od vremena za uzorke S1, S2 i S3

The decrease in the value of the corrosion potential of the tested samples can be explained by the gradual activation of the steel surface due to the action of chloride ions.

The value of the corrosion potential established at the end of the test period (> 2500 s) for S1 and S2 is approximately the same and amounts to ~ -615 mV, while in the case of S3, the value of the corrosion potential was more positive and amounted to ~ -585 mV. The more positive value of the corrosion potential for S3 is a consequence of the higher chromium content in that sample (~ 15 wt.% Cr), i.e. the presence of a passive film on its surface.

3.2. LPR measurements

The linear polarization resistance (LPR) method is a widely used electrochemical method for determining the corrosion rate of steel and other metals and alloys as well as protective systems (corrosion inhibitors and organic and inorganic coatings). Corrosion monitors that are usually used to determine the value of general corrosion and the tendency to pitting corrosion in an on-field environment are based on the LPR method.

Figure 2a-c shows the polarization diagrams *E*-*j* obtained by the LPR measurements. The slope of the curve ($\Delta E/\Delta j$) on the corrosion potential (E_{corr}) corresponds to the value of the polarization resistance (R_p). The value of polarization resistance for S1 is the lowest and the highest for S3 (Figure 2 and Table 3). The highest value R_p for S3 as can be expected is a consequence of a higher amount of chromium (~15 wt.% Cr).

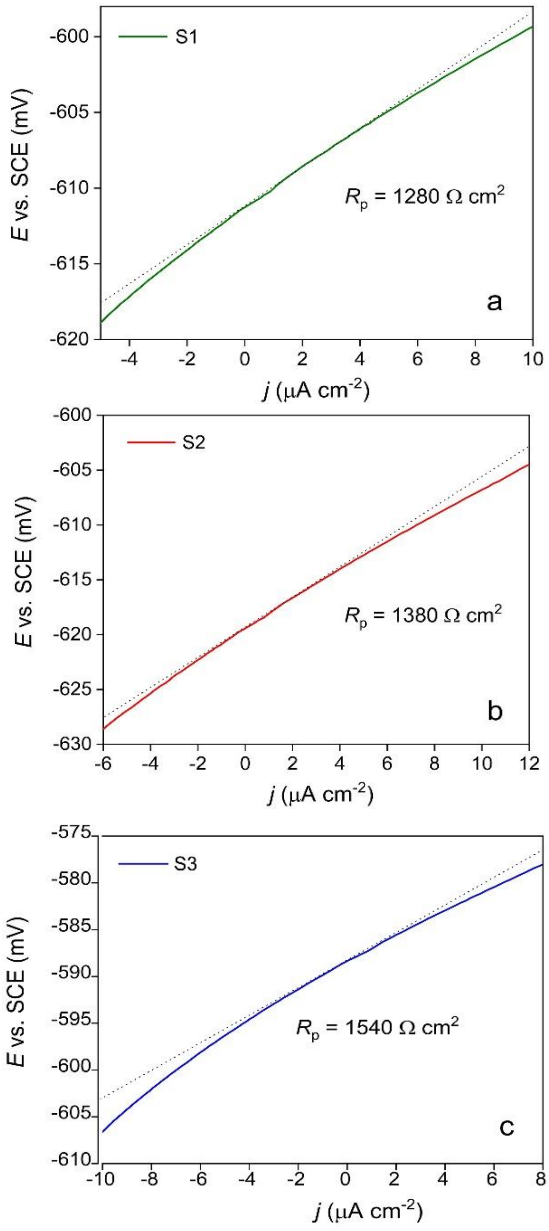

Figure 2. LPR diagrams for samples: a) S1, b) S2, and c) S3

Slika 2. LPR dijagrami za uzorke: a) S1, b) S2 i c) S3

Based on the experimental values for the polarization resistance (R_p), the corrosion current density (j_{corr}) was calculated using Equation (3). The corrosion current density is directly proportional to the corrosion rate (v_{corr}). The corrosion rate was calculated using Equation (4).

3.3. EIS measurements

Electrochemical impedance spectroscopy (EIS) has been successfully applied to the study of corrosion systems during the previous few decades and today it is considered a reliable and precise method for studying the corrosion process and determining the corrosion rate. An important advantage of this method is the possibility of applying signals of small amplitudes, which negligiblely disturb the tested metal surface.

Figure 3 summarizes the Nyquist diagrams obtained by the EIS measurements for S1, S2 and S3 in 3% NaCl solution (pH 8.1). The INSET of Figure 3 shows the Equivalent Electrical Circuit (EEC) which can be applied for the analyses of the corrosion system (tested samples/NaCl solution). On the EEC the polarization resistance is presented by R_p, the Constant Phase Element is presented by CPE, and the electrolyte resistance by R_e. The Constant Phase Element (CPE) was introduced instead of the capacity of the double layer on the surface of the tested steels (C_{dl}). The CPE contains all the microstructural inhomogeneities of the examined steel surface, such as surface roughness and segregation of alloying elements [16].

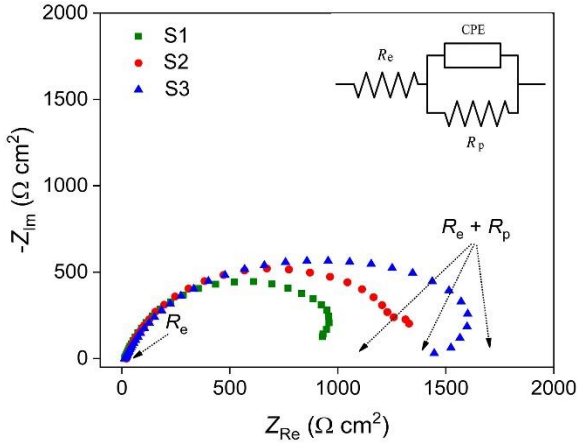

Figure 3. Nyquist diagrams obtained by the EIS method for S1, S2, and S3. INSET: Equivalent Electrical Circuit (EEC)

Slika 3. Najkvistovi dijagrami dobijeni primenom EIS metode za čelik 1, čelik 2 i čelik 3. UMETNUTO: Ekvivalentno Električno Kolo (EEC)

The larger the diameter of the semicircle on the Nyquist diagrams (Figure 3), the higher the value of the polarization resistance (R_p), that is, the greater the steel resistance to general corrosion. In the case of stainless iron (S3), the largest semicircle diameter was obtained on the Nyquist diagram.

The Nyquist plot gives the dependence of the real impedance component (Z_{Re}) and the imaginary impedance component (Z_{Im}) in linear coordinates. The electrolyte resistance value is R_e ~ 10 Ω cm^2 (Figure 3 and Figure 4a). On the right side of the Nyquist diagram, the total resistance $R_e + R_p$ is shown. Therefore, the values of polarization resistances (R_p) are ~ 1100 Ω cm^2, ~ 1400 Ω cm^2, and ~1700 Ω cm^2, for S1, S2 and S3 respectively. The values of the corrosion current density were calculated using Equation (3), and corrosion rate values using Equation (4).

Figure 4a shows a summary of the Bode modulus diagrams obtained using the EIS method for the tested samples. The Bode modulus diagram represents the dependence of the impedance modulus (Z_{Mod}) on the applied frequency (f) in logarithmic coordinates.

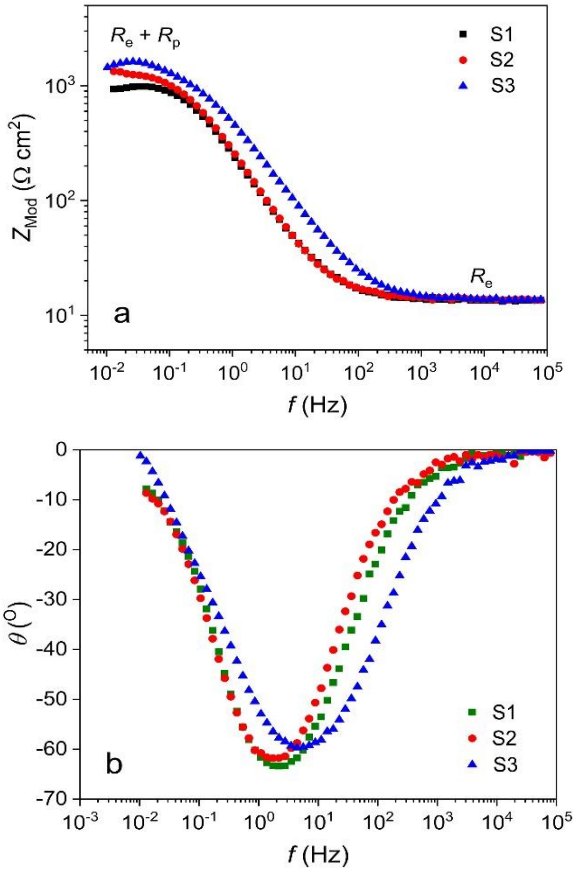

Figure 4. Bode diagrams obtained using the EIS method a) Bode modulus, and b) Bode phase diagrams, for samples S1, S2, and S3

Slika 4. Bodeovi dijagrami dobijeni primenom EIS metode a) Bode moduo, i b) Bode fazni dijagram, za uzorke: S1, S2 i S3

The Bode modulus diagrams at relatively high frequencies (from 10^3 to 10^5 Hz) are related to the electrolyte resistance (R_e), which remains constant during the measurements (R_e ~ 10 Ω cm^2). For intermediate frequency values (10^3 to 10^{-1} Hz) the Bode modulus curves for S1 and S2 overlap, while the curve for S3 (stainless cast iron) is shifted towards higher impedance values. The shift of the Bode modulus curve towards higher impedance values is also a consequence of the higher chromium content (~15 wt.% Cr) and the presence of a passive layer on the surface of that stainless iron. The plateau at low frequencies corresponds to the value of polarization resistance ($R_e + R_p$).

Figure 4b shows a summary of the Bode phase diagrams for the tested samples. The Bode phase diagram shows the dependence of the phase angle (Θ) on the logarithm of the frequency (f). The frequency at which some corrosion reaction takes place can be determined. Also, deeper interpretations of corrosion processes on the metal surface can be performed. The shape of the Bode phase diagrams for the tested samples in 3% NaCl solution (Figure 4b) indicates the existence of only one time constant, i.e. existence of one peak on the phase diagrams. The corresponding Equivalent Electrical Circuit is shown in the INSET of Figure 3.

Table 3. Summarized results of LPR and EIS methods for the tested samples

Tabela 3. Sumirani rezultati LPR i EIS metoda za ispitane čelike

	LPR		EIS	
	R_p (Ω cm^2)	v_{corr} (mm yr^{-1})	R_p (Ω cm^2)	v_{corr} (mm yr^{-1})
S1	1280	0.23	1100	0.26
S2	1380	0.21	1400	0.21
S3	1540	0.19	1700	0.17

Table 3 lists the values of polarization resistance (R_p), measured using the LPR and EIS method, as well as the values of the corrosion rate (v_{corr}), calculated using equation (4).

3.4. Linear sweep voltammetry (LSV)

Applying the LSV method, the value of the corrosion current density (j_{corr}) was determined. The value of the corrosion rate (v_{corr}) can be directly calculated by applying the Faraday law, based on corrosion current density. The disadvantage of the LSV method is relatively large polarizations (usually ± 0.25 V), and as a result, there is a significant perturbance in the metal surface (the tested samples), so the LSV method is considered a destructive method.

Summarised Tafel diagrams (obtained in a 3% NaCl solution, pH 8.1) for the tested samples are shown in Figure 5. The corrosion current density (j_{corr}) was determined by extrapolation of the anodic Tafel regions on the corrosion potential (E_{corr}). The corrosion current density value j_{corr} = 38 μA cm^{-2}, 27 μA cm^{-2}, and 23 μA cm^{-2} for S1, S2, and S3, respectively. Based on the corrosion current density, the corrosion rate (v_{corr}) can be calculated, provided that the steel corrodes uniformly.

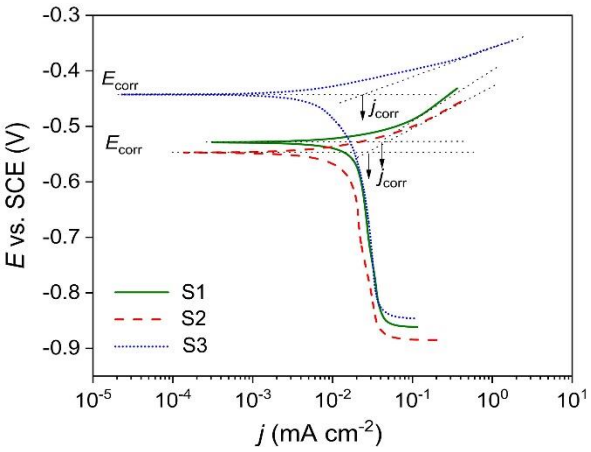

Figure 5. Tafel diagrams for samples: S1, S2, and S3, in a 3 %NaCl solution (pH 8.1).

Slika 5. Tafelovi dijagrami za uzorke: S1, S2 i S3, dobijeni u rastvoru 3% NaCl (pH 8,1).

3.5. Appearance of the surface of the samples after polarization measurements

Figure 6 shows the appearance of the steel surface after performing linear sweep voltammetry (LSV) measurements. The application of this electrochemical method involves relatively high anodic polarizations (± 0.25 V) so that intense dissolution of the steel surface can occur during testing. Dissolution of the steel surface is incomparably less when tests are performed using the LPR or EIS method.

Localized corrosion (pitting corrosion) occurred in all tested samples, after anodic polarization in a 3% NaCl solution applying the LSV method. In the case of S1 as casted steel, the pits are significantly larger than in the case of S2 (rolled steel). In the case of stainless iron (cast S3), the formed pits are of very large dimensions (several hundred micrometres) and have the form of pits with a so-called lacy cover (Figure 6). The passive film on the surface of S3 (stainless cast iron because this steel contains 15.14 wt.% Cr and 2.56 wt.% C), in a solution containing a high concentration of chloride ions (3% NaCl solution), is not stable enough under anodic polarizations, so pits are formed. Pits are formed at favourable places in the microstructure of the tested stainless steel, such as the boundaries

of MnS inclusions with the surrounding matrix, as well as on the other inhomogeneities, as liquations on the steel surface [33].

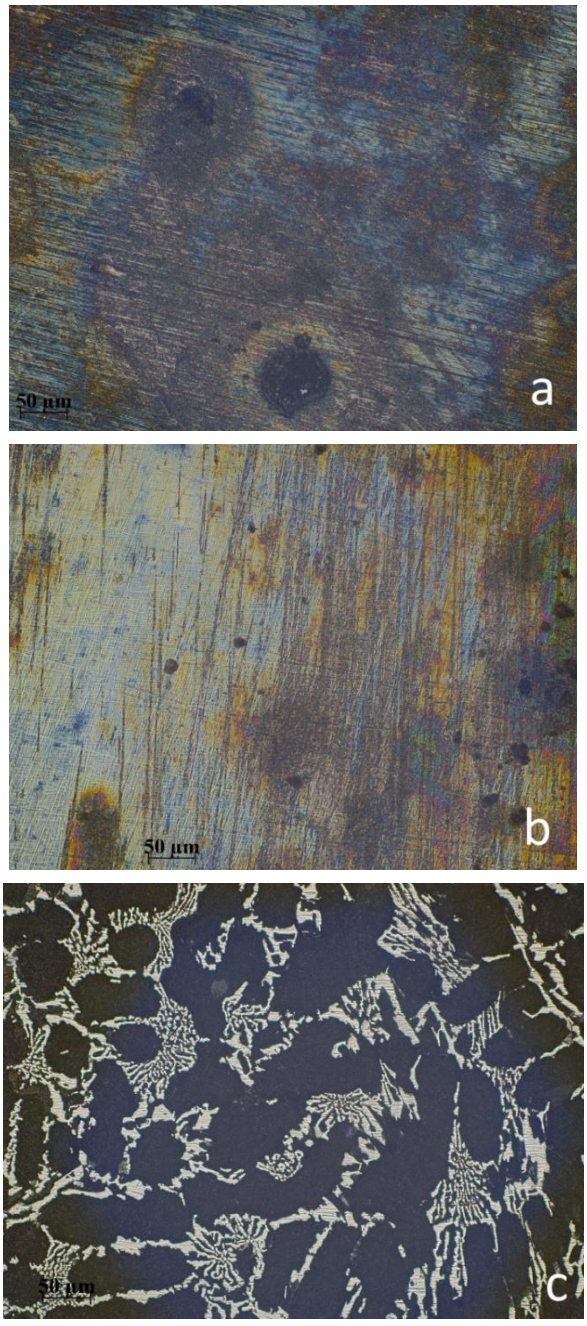

Figure 6. Appearance of samples surface after polarization measurements a) S1, b) S2, and c) S3

Slika 6. Izgled površine uzoraka nakon polarizacionih merenja: a) S1, b) S2 i c) S3

During the polarization measurements (LSV method), localized forms of corrosion (pitting corrosion) occurred, so the obtained values of the corrosion current density (j_{corr}) cannot be used to calculate the general corrosion rate (v_{corr}) of the tested samples.

4. CONCLUSION

The corrosion behaviour of different types of steel and iron that can be potentially used for making steel balls in copper and other ore grinding mills in the presence of seawater was analysed. Two steels are low-alloy carbon steels (S1 as cast, and S2 as rolled), while the third (S3) is stainless cast iron, containing ~15.14 wt.% Cr and 2.56 wt.% C. Three electrochemical methods were used to determine the corrosion rate: the linear polarization resistance (LPR) method, the electrochemical impedance spectroscopy (EIS) method and the linear sweep voltammetry (LSV) method.

Based on the results of the LPR and EIS methods (as non-destructive methods), the value of polarization resistance (R_p) was determined, and then, using the Stern-Gary equation and Faraday law, the general corrosion rate (v_{corr}) of the samples was calculated.

The obtained values for the general corrosion rate (v_{corr}) can be used to predict the service life of the steel balls in the exploitation conditions (seawater).

Using the linear sweep voltammetry (LSV) method, the corrosion current density (j_{corr}) was determined, which can be used to directly calculate the general corrosion rate (v_{corr}), using Faraday law. However, during the linear sweep voltammetry testing at relatively high anodic polarizations, localized forms of corrosion occur, such as pitting corrosion. Therefore, this method is not suitable for calculating the general corrosion rate.

Characteristic microphotographs (which show the presence of localized forms of corrosion, such as pitting corrosion) were obtained for the tested steels after performing the linear sweep voltammetry (LSV) measurements.

Acknowledgements

This study was financially supported by the Ministry of Science, Technological Development and Innovation of the Republic of Serbia (Grant No. 451-03-47/2023-01/200026 and 451-03-47/2023--01/200135).

5. LITERATURE

[1] Standard Guide for Determining Synergism Between Wear and Corrosion: ASTM G119-2009. https://doi.org/10.1520/G0119-09.

[2] E.McCafferty (2010) Introduction to Corrosion Science, Springer, New York

[3] L.Yang (2021) Techniques for corrosion monitoring, Cambridge, England

[4] R.Baboian (2005) ASTM Corrosion Tests and Standards: Application and Interpretation, second ed., ASTM International

[5] Standard Guide for Conducting Corrosion Tests in Field Applications, ASTM G4-2014. https://doi.org/10.1520/G0004-01R14.

[6] Standard Practice for Conducting Atmospheric Corrosion Tests on Metals, ASTM G50-2015. https://doi.org/10.1520/G0050-10R15.

[7] K.Chiang, T.Mintz (2021) Gravimetric techniques, in Techniques for corrosion monitoring,Edited by L.Yang, Cambridge, England, p.239-254.

[8] Standard Guide for Laboratory Immersion Corrosion Testing of Metals, ASTM G31-2012. https://doi.org/10.1520/G0031-12A.

[9] Standard Practice for Exposure of Metals and Alloys by Alternate Immersion in Neutral 3.5 % Sodium Chloride Solution, ASTM G44-2013. https://doi.org/10.1520/G0044-99R13.

[10] Corrosion tests in artificial atmospheres-Salt spray tests: ISO 9227-2017.

[11] F.Mansfeld (1976) The Polarisation Resistance Technique for Measuring Corrosion Currents, in Advances in Corrosion Science and Technology, Vol. 6, Edited M.G.Fontana and R.W.Staehle, Plenum Press, New York and London, p.163-262.

[12] J.R.Scully (2000) Polarization resistance methods for determination of instantaneous corrosion rates, Corrosion, 56(2), 199-218. https://doi.org/10.5006/1.3280536

[13] Standard Test Method for Conducting Potentiodynamic Polarization Resistance Measurements, ASTM G59-2014. https://doi.org/10.1520/G0059-97R14.

[14] R.G.Kelly, J.R.Scully, D.W.Shoesmith, R.G. Buchheit (2002) Electrochemical Techniques in Corrosion Science and Engineering, Marcell Dekker, New York

[15] M.E.Orazem, B.Tribollet (2017) Electrochemical Impedance Spectroscopy, John Wiley &Sons, New Jersey

[16] R.Srinivasan, F.Fasmin (2021) An Introduction to Electrochemical Impedance Spectroscopy, Taylor & Francis Group, New York

[17] F.Mansfeld (2006) Electrochemical Impedance Spectroscopy, in Analytical Methods in Corrosion Science and Engineering, Edited By P. Marcus and F. Mansfeld, Taylor & Francis Group, p.463-505.

[18] Standard Practice for Verification of Algorithm and Equipment for Electrochemical Impedance Measurements, ASTM G106-2015. https://doi.org/10.1520/G0106-89R15.

[19] S. Papavinasam (2021) Electrochemical polarization techniques for corrosion monitoring, Techniques for corrosion monitoring, Edited by L.Yang, Cambridge, England, p.45-75.

[20] E. Heitz (2006) DC Electrochemical Methods, in Analytical Methods, in Corrosion Sciencen and Engineering, Edited By P.Marcus and F.Mansfeld, Taylor & Francis Group, p.435-462.

[21] F. Mansfeld (2003) Electrochemical methods of corrosion testing, in: ASM Handbook, Vol. 13A, Corrosion: Fundamentals, Testing and Protection, ASM International, p.446-462.

[22] E.E.Stansbury, R.A. Buchanan (2000) Fundamentals of Electrochemical Corrosion, ASM International, Materials Park, Ohio

[23] E. Bardal (2004) Corrosion and protection, Springer, London, Berlin, New York

[24] Standard Test Method for Corrosion Potentials of Uncoated Reinforcing Steel in Concrete, ASTM-C876-2009. https://doi.org/10.1520/C0876-09.

[25] Standard Guide for Development and Use of a Galvanic Series for Predicting Galvanic Corrosion Performance, ASTM G82-2014. https://doi.org/10.1520/ G0082-98R14.

[26] Standard Test Method for Measurement of Corrosion Potentials of Aluminum Alloys1ASTM G69-2012. https://doi.org/10.1520/G0069-12.

[27] Test Method for Standard Test Method for Evaluating the Potential for Galvanic Corrosion for Medical Implants, ASTM F3044-2014. https://doi.org/ 10.1520/F3044-14.

[28] Standard Guide for Electrode Potential Measurement, ASTM G215-2016.https://doi.org/10.1520/G0215-16.

[29] B.V.Jegdić, B.M.Bobić, M.Bošnjakov (2017) Relationship between corrosion potential and different corrosion forms of metals, alloys and theirs welded joints - part I, Welding and Welded Structures, 62(2), 65-76. https://doi.org/10.5937/zzk1702065J

[30] B.V.Jegdić, B.M. Bobić, B.M. Radojković (2018) Relationship between corrosion potential and different corrosion forms of metals, alloys and theirs welded joints - part II, Welding and Welded Structures, 63(2), 53-63. https://doi.org/10.5937/zzk1802053J

[31] M.Stern, A.L.Geary (1957) Electrochemical polarization. I. A theoretical analysis of the shape of the polarization curves, Journal of The Electrochemical Society, 104(1), 56-63. https://doi.org/10.1149/1.2428473

[32] Standard Practice for Calculation of Corrosion Rates and Related Information from Electrochemical Measurements, ASTM G102-2015.

[33] B.Radojković, B.Jegdić, J.Pejić, D.Marunkić, A.Simović, S.Eraković-Pantović (2023) Influence of nitrogen content on the pit formation and pit propagation in the welded joints of X5CrNi18-10 stainless steel, Materiales Corrosion (accepted). https://doi.org/10.1002/maco.202314120

IZVOD

KOROZIONO PONAŠANJE ČELIČNIH KUGLICA ZA MLEVENJE SA VISOKIM I NISKIM SADRŽAJEM HROMA U RASTVORU HLORIDA

Ispitivano je koroziono ponašanje tri vrste legura (dva nisko-legirana ugljenična čelika i jedan uzorak je nerđajuće gvožđe sa ~15% Cr), u rastvoru koji simulira morsku vodu (3% rastvor NaCl, pH 8,1). Ispitani uzorci se koriste za proizvodnju čeličnih kugli koje se primenjuju u mlinovima za mlevenje bakarnih i drugih ruda. Koroziona ispitivanja su izvedena primenom tri elektrohemijske metode, na sobnoj temperaturi u prisustvu atmosferskog kiseonika. Korišćene su metoda linearne polarizacione otpornosti (LPR), metoda elektrohemijske impedansne spektroskopije (EIS) i metoda linearne promene potencijala (LSV). Na osnovu merenja LPR i EIS metodama (kao nerazarajućim metodama), određena je vrednost polarizacione otpornosti (R_p), a zatim je izračunata vrednost brzine opšte korozije (v_{kor}) ispitivanih uzoraka. Dobijene vrednosti za brzinu opšte korozije se mogu koristiti za izračunavanje veka trajanja kugli u uslovima eksploatacije (morska voda). Izgled površine ispitivanih uzoraka nakon izvođenja LSV metode pokazao je prisustvo lokalizovane korozije (formirane su jamice, pitovi) na ispitivanim uzorcima, posebno na nerđajućem gvožđu. Prema tome, LSV metoda nije pogodna za određivanje brzine opšte korozije ispitivanih čelika u morskoj vodi. Ovaj oblik korozije javlja se pri visokim anodnim polarizacijama tokom izvođenja LSV merenja.

Ključne reči: *Nisko-legirani čelik, nerđajuće gvožđe, elektrohemijska korozija, LPR, EIS, LSV, morska voda*

Naučni rad

Rad primljen: 14.09.2023.

Rad prihvaćen: 12.10.2023.

Rad je dostupan na sajtu: www.idk.org.rs/casopis